

Impact of channel fluctuations on channel estimation performance in the underwater acoustic environment

Zheng Guo, and Aijun Song

Citation: *Proc. Mtgs. Acoust.* **39**, 070004 (2019); doi: 10.1121/2.0001272

View online: <https://doi.org/10.1121/2.0001272>

View Table of Contents: <https://asa.scitation.org/toc/pma/39/1>

Published by the [Acoustical Society of America](#)

ARTICLES YOU MAY BE INTERESTED IN

[Machine learning in acoustics: Theory and applications](#)

The Journal of the Acoustical Society of America **146**, 3590 (2019); <https://doi.org/10.1121/1.5133944>

[Impact of channel fluctuations on channel estimation errors in underwater acoustic communications](#)

The Journal of the Acoustical Society of America **146**, 2763 (2019); <https://doi.org/10.1121/1.5136567>

[Sparse direct adaptive equalization based on proportionate recursive least squares algorithm for multiple-input multiple-output underwater acoustic communications](#)

The Journal of the Acoustical Society of America **148**, 2280 (2020); <https://doi.org/10.1121/10.0002276>

[Experimental analysis of the effects of bistatic target scattering on synthetic aperture sonar imagery](#)

Proceedings of Meetings on Acoustics **39**, 070001 (2019); <https://doi.org/10.1121/2.0001248>

[Designing a waveguide to transmit sound to a dolphin in a functional magnetic response imaging machine](#)

Proceedings of Meetings on Acoustics **39**, 010001 (2019); <https://doi.org/10.1121/2.0001282>

[Session Summary of "Parabolic Equation Methods Across Acoustics"](#)

Proceedings of Meetings on Acoustics **39**, 002001 (2019); <https://doi.org/10.1121/2.0001277>



**Advance your science and career
as a member of the**

ACOUSTICAL SOCIETY OF AMERICA

LEARN MORE





178th Meeting of the Acoustical Society of America

San Diego, CA

2-6 December 2019

Underwater Acoustics: Paper 1aUW3

Impact of channel fluctuations on channel estimation performance in the underwater acoustic environment

Zheng Guo

*Department of Electrical and Computer Engineering, University of Alabama, Tuscaloosa, AL, 35487;
zguo18@crimson.ua.edu*

Aijun Song

University of Alabama, Tuscaloosa, AL, 35487; song@eng.ua.edu

Channel estimation is critical to achieve high data rate acoustic communications in the ocean. Channel estimates are often utilized to address the distortions induced by multipath propagation in various communication receivers. Therefore, accurate channel estimation is often the prerequisite for reliable coherent acoustic communications. Many efforts have been devoted to either characterizing the acoustic channel or developing high-performance channel estimation algorithms. However, limited work has been directed to investigate effect of channel fluctuations on estimation performance. Here we seek to quantify the impact of channel fluctuations on least squares channel estimators. A new metric, channel variation ratio, is used to describe the rate of fluctuations in the acoustic impulse responses. We investigate the relationship between the mean squared error (MSE) of the channel estimates and the channel variation ratio. We show the new metric can be used to predict channel estimation MSE for least squares channel estimators. Numeric results also show that there exists an optimal channel length with the minimum estimation error for fluctuating acoustic channels. Both computer simulations and experimental data have been used to validate the findings.

1. INTRODUCTION

Channel estimation is critical to achieve high data rate acoustic communications in the ocean. Channel estimates are often utilized to address the distortions induced by multipath propagation in various communication receivers. Therefore, accurate channel estimation is often the prerequisite for reliable coherent acoustic communications.

Many efforts have been devoted to either characterizing the acoustic channel or developing high-performance channel estimation algorithms. Ref. [1] models the channel by the combination of a pseudo-coherent component and pseudo-deterministic component. This model infers that the channel is trend stationary during the observation windows of a few minutes. Ref. [2] confirms that the random component in the channel can be well approximated by the zero-mean Gaussians distribution. Ref. [3] characterizes channel fluctuations using the coherent-to-incoherent intensity ratio. This metric can provide a metric measuring the stability of each channel tap. Ref. [4] formulates the received signal using time varying channel. The authors propose an adaptive subspace-tracking with a reduced-rank estimation algorithm for time-varying channels. Ref. [5] models the received signal based on the delay-Doppler spread function. Delay-Doppler functions, instead of channel impulse responses, are estimated in fast time-varying sparse channel conditions.

Limited work has been directed to investigate effect of channel fluctuations on estimation performance. Ref. [6] observes that the communications performance varies when different lengths of estimated impulse responses are used in the time-reversal receiver based on experimental data. Ref. [7] uses channel estimation errors to predict passive phase conjugation receiver performance, based on the piecewise-fixed channel assumption. Ref. [8] finds that channel estimation errors need to be incorporated to predict communication performance when replaying experimental data. The effects of fast channel variations on channel estimation have not studied.

Here we seek to quantify the impact of channel fluctuations on least squares channel estimators. A new metric, channel variation ratio, is used to describe the rate of fluctuations in the acoustic impulse responses. We investigate the relationship between the mean squared error (MSE) of the channel estimates and the channel variation ratio. We show the new metric can be used to predict channel estimation MSE for least squares channel estimators. Numeric results also show that there exists an optimal channel length with the minimum estimation error for fluctuating acoustic channels. Both computer simulations and experimental data have been used to validate the findings.

2. CHANNEL VARIATION RATIO

We define the channel vector $\mathbf{h}[n]$ as the channel impulse responses at instant n , i.e.,

$$\mathbf{h}[n] = (h[n; 0], h[n; 1], \dots, h[n; L - 1])^T. \quad (1)$$

where L is the channel length.

We split the channel vector into two parts, time-invariant and time-variant components. That is,

$$\mathbf{h}[n] = \mathbf{h}_i[n] + \mathbf{h}_v[n], \quad (2)$$

where $\mathbf{h}_i[n]$ is the time-invariant component, $\mathbf{h}_v[n]$ is time-variant component independent of $\mathbf{h}_i[n]$.

Based on the channel model above, we define the channel variation ratio (CVR) as the the intensity ratio between the time-variant component and the entire channel,

$$\gamma = \frac{E[\|\mathbf{h}_v[n]\|_2^2]}{E[\|\mathbf{h}[n]\|_2^2]} = \frac{E[\|\mathbf{h}_v[n]\|_2^2]}{\|\mathbf{h}_i\|_2^2 + E[\|\mathbf{h}_v[n]\|_2^2]}. \quad (3)$$

where $E[\cdot]$ denotes the expectation operation and $\|\cdot\|_2^2$ denotes l_2 -norm.

The CVR is defined over a context period of T . The period, T , should be tens of milliseconds or seconds at most.

3. LINKING THE CVR WITH CHANNEL ESTIMATION PERFORMANCE METRICS

The received signal is

$$\begin{aligned} \mathbf{r} &= \mathbf{H}\mathbf{s} + \mathbf{w} \\ &= \mathbf{S}\mathbf{h}_i + \mathbf{H}_v\mathbf{s} + \mathbf{w}, \end{aligned} \quad (4)$$

where \mathbf{H} is the channel convolution matrix, \mathbf{s} is the transmitted symbols, \mathbf{w} is the additive white Gaussian noise with a variance of σ_w^2 . The reception is the convolution of the channel and transmitted symbols, with the additive white Gaussian noise. This can also be expressed in a matrix form as in the second line of Eq. 4, where $\mathbf{H}\mathbf{s}$ is split into two parts. \mathbf{S} is the symbol convolution matrix constructed by \mathbf{s} , \mathbf{H}_v is represented by

$$\mathbf{H}_v = \begin{bmatrix} h_v[0; L-1] & h_v[0; L-2] & \cdots & h_v[0; 0] & 0 & \cdots & 0 \\ 0 & h_v[1; L-1] & h_v[1; L-2] & \cdots & h_v[1; 0] & \cdots & 0 \\ \vdots & \ddots & \ddots & \ddots & \cdots & \ddots & \vdots \\ 0 & \cdots & 0 & h_v[M; L-1] & h_v[M; L-2] & \cdots & h_v[M; 0] \end{bmatrix}, \quad (5)$$

where M is the length of the observation window.

To quantify the performance of channel estimation, we use two metrics: mean squared error (MSE) and signal prediction error (SPE). The MSE is defined as

$$\delta = E\left[\frac{1}{q} \sum_{n=0}^{q-1} \|\hat{\mathbf{h}} - \mathbf{h}\|_2^2\right], \quad (6)$$

where $\hat{\mathbf{h}}$ is the channel estimate, q is the number of varying channels during the context window T .

The SPE is defined as

$$\zeta = E[\|\hat{\mathbf{r}} - \mathbf{r}\|_2^2], \quad (7)$$

where $\hat{\mathbf{r}}$ is the estimation of \mathbf{r} .

We only consider least square channel estimator here. Thus $\hat{\mathbf{h}} = \mathbf{S}^\dagger \mathbf{r}$ where \mathbf{S}^\dagger is the pseudo-inverse of \mathbf{S} . We get the MSE expression as a function of the CVR,

$$\delta = \frac{\gamma}{1-\gamma} \|\mathbf{h}_i\|_2^2 - 2E\left[\frac{1}{q} \sum_{n=0}^{q-1} (\mathbf{h}_v^H \mathbf{S}^\dagger \mathbf{H}_v \mathbf{s})\right] + E[\|(\mathbf{S}^\dagger \mathbf{H}_v \mathbf{s})\|_2^2] + E[\text{trace}((\mathbf{S}^\dagger)^H \mathbf{S}^\dagger)] \sigma_w^2. \quad (8)$$

We observe from Eq. 8 that the MSE changes with $\frac{\gamma}{1-\gamma} \|\mathbf{h}_i\|_2^2$ and the noise power σ_w^2 . The MSE approaches zero only when the CVR and noise power are both zeros.

We can also obtain the the expression of the SPE as

$$\begin{aligned} \zeta &= E[\|(\mathbf{H}_v \mathbf{s})\|_2^2] - 2E[(\mathbf{H}_v \mathbf{s})^H \mathbf{S} \mathbf{S}^\dagger \mathbf{H}_v \mathbf{s}] + E[\|(\mathbf{S} \mathbf{S}^\dagger \mathbf{H}_v \mathbf{s})\|_2^2] \\ &\quad + (1 - 2E[\text{trace}(\mathbf{S} \mathbf{S}^\dagger)] + E[\text{trace}((\mathbf{S} \mathbf{S}^\dagger)^H \mathbf{S} \mathbf{S}^\dagger)]) \sigma_w^2. \end{aligned} \quad (9)$$

Considering the truncation effect [7], we rewrite Eq. 4 as

$$\mathbf{r} = \mathbf{S}_{tr} \mathbf{h}_{tr} + \mathbf{S}_{res} \mathbf{h}_{res} + \mathbf{H}_v \mathbf{s} + \mathbf{w}, \quad (10)$$

where $\mathbf{S} = \mathbf{S}_{tr} + \mathbf{S}_{res}$, \mathbf{S}_{tr} is the symbol convolution matrix after truncation, and \mathbf{S}_{res} is the residue. $\mathbf{h}_i = \mathbf{h}_{tr} + \mathbf{h}_{res}$, \mathbf{h}_{tr} is the impulse response after truncation and \mathbf{h}_{res} is the residue.

Taking effects from both channel fluctuations and truncation, we rewrite Eq. 8 as

$$\begin{aligned} \delta = & \frac{\gamma}{1-\gamma} \|\mathbf{h}_i\|_2^2 + E[\|(\mathbf{S}_{tr}^\dagger \mathbf{S}_{res} \mathbf{h}_{res})\|_2^2] + E[\text{trace}((\mathbf{S}_{tr}^\dagger)^H \mathbf{S}_{tr}^\dagger)] \sigma_w^2 \\ & + E[\|(\mathbf{S}_{tr}^\dagger \mathbf{H}_v \mathbf{s})\|_2^2] - 2E[\frac{1}{q} \sum_{n=0}^{q-1} (\mathbf{h}_v^H \mathbf{S}_{tr}^\dagger \mathbf{H}_v \mathbf{s})] + \|\mathbf{h}_{res}\|_2^2 - 2E[\mathbf{h}_{res}^H \mathbf{S}_{tr}^\dagger \mathbf{S}_{res} \mathbf{h}_{res}], \end{aligned} \quad (11)$$

where \mathbf{S}_{tr}^\dagger is the pseudo-inverse of \mathbf{S}_{tr} .

Similarly, we reformulate Eq. 9 as

$$\begin{aligned} \zeta = & E[\|\mathbf{S}_{res} \mathbf{h}_{res}\|_2^2] - 2E[(\mathbf{S}_{res} \mathbf{h}_{res})^H \mathbf{S}_{tr} \mathbf{S}_{tr}^\dagger \mathbf{S}_{res} \mathbf{h}_{res}] + E[\|\mathbf{S}_{tr} \mathbf{S}_{tr}^\dagger \mathbf{S}_{res} \mathbf{h}_{res}\|_2^2] \\ & + E[\|\mathbf{H}_v \mathbf{s}\|_2^2] - 2E[(\mathbf{H}_v \mathbf{s})^H \mathbf{S}_{tr} \mathbf{S}_{tr}^\dagger \mathbf{H}_v \mathbf{s}] + E[\|\mathbf{S}_{tr} \mathbf{S}_{tr}^\dagger \mathbf{H}_v \mathbf{s}\|_2^2] \\ & + (1 - 2E[\text{trace}(\mathbf{S}_{tr} \mathbf{S}_{tr}^\dagger)] + E[\text{trace}((\mathbf{S}_{tr} \mathbf{S}_{tr}^\dagger)^H \mathbf{S}_{tr} \mathbf{S}_{tr}^\dagger)]) \sigma_w^2. \end{aligned} \quad (12)$$

With the introduction of channel truncation effect, we can see both MSE and SPE change with the truncated channel power also.

4. SIMULATIONS

Simulations were conducted to verify the correctness of the MSE and SPE expressions. For the case of static channel, the used channel impulse response is shown in Fig. 1. The channel was extracted from an experiment, which will be described in Sec. 5.

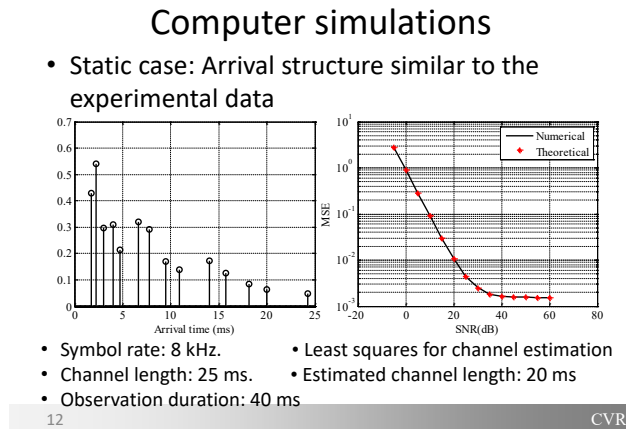


Figure 1: Static channel impulse response.

We computed the MSEs under different signal to noise ratios (SNR). The SNRs ranged from -5 dB to 60 dB. Fig. 1 clearly indicate that the error floor decreased when the SNR increased.

We simulated a time-varying channel as shown in Fig. 2. Corresponding error floor using MSE has been computed with different SNRs. Results are presented in Fig. 3. We can see from Fig. 3 that the MSE with channel fluctuation is higher than that in Fig. 1.

We then combined channel variation and truncation, and computed the MSE and SPE. Corresponding results are shown in Fig. 4. Both MSE and SPE decreased when the channel length increased. After reaching the minimum point, both of them increased with the channel length. We can tell from Fig. 4 that there is an optimal channel length with minimum MSE and SPE. The optimal channel length here is 20 ms.

Time-varying cases

- Time-varying impulse responses with CVR=0.1 [T=1 s]

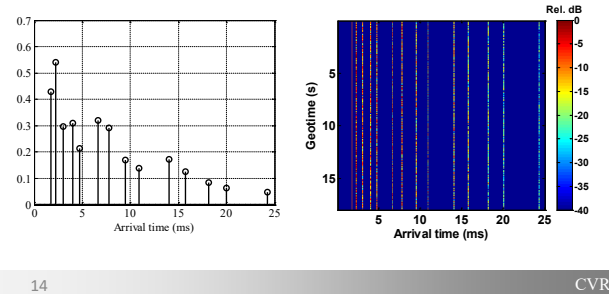


Figure 2: Time-varying channel impulse responses.

Error floor from channel variability

- CVR=0.1 [T=1 s]

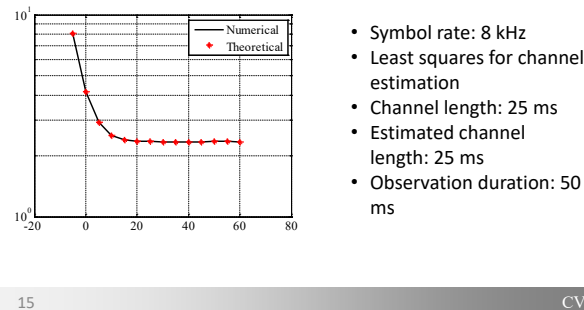


Figure 3: MSE floor for the time-varying case.

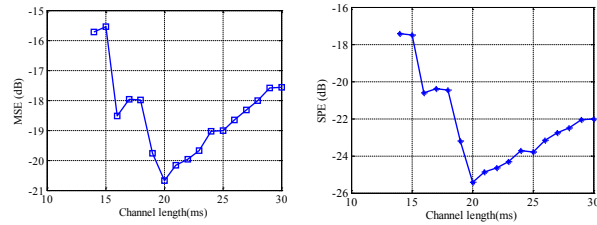
5. EXPERIMENT

We used experimental data to validate our theoretical analysis. The experiment was described in Ref. [9]. The water depth was 20 m. The transducer was mounted at the depths of 10 m. The receiver was deployed at the depth of about 16 m. The measured channel impulse response is shown in Fig. 5. The SPE were calculated using different channel lengths, from 15 to 40 ms.

We extracted the multipath structure from the measured channel. A time varying channel component was added based on the channel model in Eq. 2. The comparison of the experimental channel and simulated channel is shown in Fig. 6. Based on the simulated channel, we computed the MSE and SPE. Results are shown in Fig. 7. The trend of SPE shown in Fig. 7 is similar to that in Fig. 4. Both simulation and experimental results have an optimal channel length of around 20 ms. The results, again, validate our analysis that there exists an optimal channel length with minimum channel estimation error.

MSE & SPE vs channel length

- SNR: 54 dB, CVR=0.4 [T=1 s]



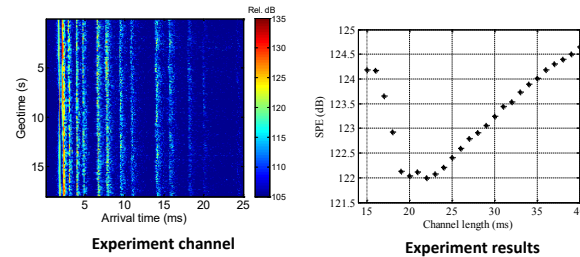
16

CVR

Figure 4: MSE floor with both channel variation and truncation effect.

Impulse responses @range=250 m

Tx @ 12 m; Rx @ 12.5 m; BPSK transmissions @ 85 kHz;
 Received signal strength: 134.6 dB; Received SNR: 54 dB
 Symbol rate: 8 kHz



18

CVR

Figure 5: Channel and SPE from experiment.

6. CONCLUSION

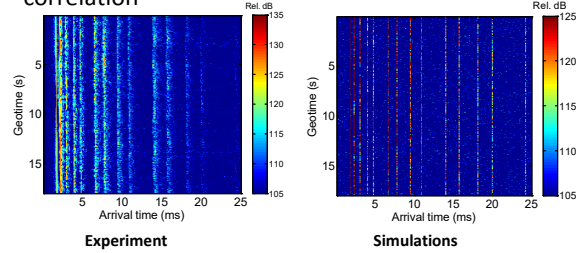
We proposed the CVR to quantify the rate of channel fluctuations. Based on the two metrics, we formulated the impacts of channel variability on channel estimation performance. We linked the CVR with channel estimation performance with two metrics, the MSE and SPE. We also analyzed impacts of channel truncation on channel estimation performance. We conclude that the CVR can be used to predict the channel estimation performance. Based on the experimental data analysis, we found there exist an optimal channel length with the minimum estimation error for fluctuating acoustic channels.

ACKNOWLEDGMENTS

The efforts presented in this paper were partly supported by the NSF (CNS-1704097, CNS-1704076).

Impulse responses @range=250 m

Match with the arrival structure and tap auto-correlation



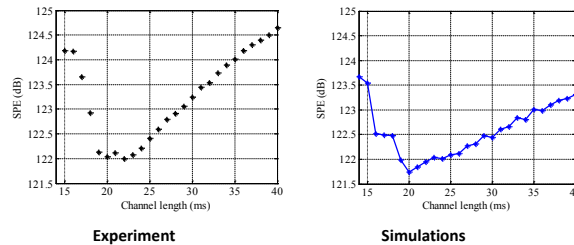
20

CVR

Figure 6: Channel comparison between experimental and simulated channel.

SPE vs channel length

• CVR=0.4 [T=1] in simulations



21

CVR

Figure 7: MSE and SPE from experiment.

REFERENCES

- [1] F. X. Socheleau, J. M. Passerieux, and C. Laot. Characterisation of time-varying underwater acoustic communication channel with application to channel capacity. In *Underwater Acoustic Measurements*.
- [2] F. X. Socheleau, C. Laot, and J. M. Passerieux. Stochastic replay of non-wssus underwater acoustic communication channels recorded at sea. *IEEE Transactions on Signal Processing*, 59(10):4838–4849, 2011.
- [3] S. H. Huang, T. C. Yang, and C. F. Huang. Multipath correlations in underwater acoustic communication channels. *The Journal of the Acoustical Society of America*, 133(4):2180–2190, 2013.
- [4] S. H. Huang, T. C. Yang, and W. Xu. Tracking channel variations in a time-varying doubly-spread underwater acoustic channel. In *MTS/IEEE Washington, October 19-22, 2015, OCEANS 2015 - MTS/IEEE Washington*. Institute of Electrical and Electronics Engineers Inc.
- [5] W. Li and J. C. Preisig. Estimation of rapidly time-varying sparse channels. *IEEE Journal of Oceanic Engineering*, 32(4):927–939, 2007.

- [6] D. Rouseff, M. Badiey, and A. Song. Effect of reflected and refracted signals on coherent underwater acoustic communication: Results from the kauai experiment (kauaiex 2003). *The Journal of the Acoustical Society of America*, 126(5):2359–2366, 2009.
- [7] J. A. Flynn, J. A. Ritcey, D. Rouseff, and W. L J. Fox. Multichannel equalization by decision-directed passive phase conjugation: Experimental results. *IEEE Journal of Oceanic Engineering*, 29(3):824–836, 2004.
- [8] G. Deane, J. C Preisig, and A. C. Singer. Making the most of field data to support underwater acoustic communications R&D. In *2018 Fourth Underwater Communications and Networking Conference (UComms)*, pages 1–5. IEEE.
- [9] Y. Zhou, A. Song, and F. Tong. Underwater acoustic channel characteristics and communication performance at 85 khz. *The Journal of the Acoustical Society of America*, 142(4):EL350–EL355, 2017.